Class Sigma Glutathione Transferase Unfolds via a Dimeric and a Monomeric Intermediate: Impact of Subunit Interface on Conformational Stability in the Superfamily†

Julie M. Stevens,‡ Judith A. T. Hornby,‡ Richard N. Armstrong,§ and Heini W. Dirr*,‡

Protein Structure−Function Research Programme, Department of Biochemistry, University of the Witwatersrand, Johannesburg, 2050, South Africa, and Department of Biochemistry and Center in Molecular Toxicology, Vanderbilt University School of Medicine, Nashville, Tennessee 37232

Received May 6, 1998; Revised Manuscript Received August 24, 1998

ABSTRACT: Solvent-induced equilibrium unfolding of a homodimeric class sigma glutathione transferase (GSTS1-1, EC 2.5.1.18) was characterized by tryptophan fluorescence, anisotropy, enzyme activity, 8-anilino-1-naphthalenesulfonate (ANS) binding, and circular dichroism. Urea induces a triphasic unfolding transition with evidence for two well-populated thermodynamically stable intermediate states of GSTS1-1. The first unfolding transition is protein concentration independent and involves a change in the subunit tertiary structure yielding a partially active dimeric intermediate (i.e., $N_2 \leftrightarrow I_2$). This is followed by a protein concentration dependent step in which I_2 dissociates into compact inactive monomers (M) displaying enhanced hydrophobicity. The third unfolding transition, which is protein concentration independent, involves the complete unfolding of the monomeric state. Increasing NaCl concentrations destabilize N_2 and appear to shift the equilibrium toward I_2 whereas the stability of the monomeric intermediate M is enhanced. The binding of substrate or product analogue (i.e., glutathione or *S*-hexylglutathione) to the protein's active site stabilizes the native dimeric state (N_2), causing the first two unfolding transitions to shift toward higher urea concentrations. The stability of M was not affected. The data implicate a region at/near the active site in domain I (most likely α-helix 2) as being highly unstable/flexible which undergoes local unfolding, resulting initially in I_2 formation followed by a disruption in quaternary structure to a monomeric intermediate. The unfolding/refolding pathway is compared with those observed for other cytosolic GSTs and discussed in light of the different structural features at the subunit interfaces, as well as the evolutionary selection of this GST as a lens crystallin.

A large number of equilibrium unfolding studies have revealed that many proteins unfold by two-state cooperative processes and that although numerous compact denatured states (molten globules) have been reported (*1*), thermodynamically stable intermediates are rarely detected (*2*). Many protein folding studies have been done on small monomeric proteins for simplicity and application of the derived principles to the protein folding problem. Cooperative unfolding transitions may be expected for single-domain monomeric proteins, but more complex pathways may be anticipated for multi-domain oligomeric proteins. Equilibrium denaturation studies of such proteins provide valuable information on the autonomous folding of domains, the relationship of folding and oligomerization processes, and determination of the thermodynamic significance of subunit interface interactions. Conformational stabilities [$\Delta G(H_2O)$][1] of monomeric proteins range between 6 and 14 kcal mol^{-1} while dimeric proteins have significantly greater stabilities (10−27 kcal mol^{-1}) (*3*).

Glutathione transferases (EC 2.5.1.18) are a supergene family of dimeric multifunctional detoxification proteins (M_r ∼50 000). GSTs catalyze the addition of reduced glutathione (GSH) to a variety of physiological and xenobiotic electrophiles (*4*) and are involved in the binding of various compounds for storage and transport (*5*). GSTs are found in most aerobic organisms and are classified in several species-independent gene classes, namely, alpha, mu, pi [as reviewed (*6*)], kappa (*7*), sigma (*8*), and theta (*9*). Three-dimensional crystal structures have been elucidated for several GST isoenzymes from various classes (for reviews, see *6*, *10*), and these reveal a conserved overall folding topology. Each subunit comprises two structurally distinct domains: the smaller N-terminal domain I containing most of the residues

† This work was supported by the University of the Witwatersrand, the South African Foundation for Research Development, Fogarty International Research Collaboration Award TW00779, and Grant GM30910 from the National Institutes of Health.

* To whom correspondence should be addressed. E-mail: 089dirr@cosmos.wits.ac.za. Fax: +27 11 716 4479.

‡ University of the Witwatersrand.

§ Vanderbilt University School of Medicine.

[1] Abbreviations: ANS, 8-anilino-1-naphthalenesulfonate; ΔASA, change in solvent-accessible surface area; CD, circular dichroism; CDNB, 1-chloro-2,4-dinitrobenzene; DTT, dithiothreitol; $\Delta G(H_2O)$, free energy of unfolding in the absence of denaturant; GdmCl, guanidinium chloride; GSH, reduced glutathione; G-site, glutathione-binding site; GST, glutathione *S*-transferase; GSTS1-1, homodimeric squid class sigma glutathione *S*-transferase; SEC-HPLC, size-exclusion high-performance liquid chromatography; S-hexylGSH, *S*-hexylglutathione; Sj26GST, 26 kDa GST from *Schistosoma japonicum*.

10.1021/bi981044b CCC: $15.00
Published on Web 10/16/1998

involved in the glutathione-binding site (G-site), together with an interaction with an aspartate on domain II of the adjacent subunit. GSTs provide a useful model for studying stability and folding within a well-characterized superfamily of proteins with conserved overall structures and diverse functional properties.

The characteristics and crystal structure of the homodimeric class sigma GST from the squid digestive gland (GSTS1-1) reveal a number of significant structural and functional differences compared with the other GST classes (*8*, *11*) (Figure 1). The interactions at the subunit interface of GSTS1-1 are predominantly hydrophilic compared with the more hydrophobic nature of the interfaces of the alpha, mu, and pi class GSTs. Furthermore, the class sigma GST lacks the prominent hydrophobic lock-and-key interaction conserved at the subunit interface of the alpha, mu, and pi classes. The lock comprises a phenylalanine/tyrosine side chain at the end of α-helix 2 of domain I which fits into a hydrophobic pocket between α-helices 4 and 5 of domain II of the neighboring subunit. Equilibrium unfolding studies with GSTs from class pi (*13*, *14*), *Schistosoma japonicum* (*15*), and class alpha (*16*) have shown that these dimeric proteins unfold via a two-state pathway in which only folded dimers or unfolded monomers are detectable at equilibrium. This suggests that the dimeric structure stabilizes the tertiary structure of the individual subunits and each of the two domains of the subunit. The issue of stability is of particular importance for the class sigma GST because it has been selected by evolution as a soluble lens refractory protein (S-crystallin) in cephalopods (*17*). Crystallins are expected to have high thermodynamic stability because of the low protein turnover in the fiber cells of the eye lens. An investigation of the folding and stability properties of an evolutionary progenitor, the class sigma GST, compared with other GSTs, provides insight into the requirements and implications of molecular evolutionary selection.

Considering the unique structural features of the class sigma GSTS1-1, and in particular those at the subunit interface, an equilibrium denaturation study was undertaken to investigate the impact of these features on unfolding/refolding and conformational stability. The squid GSTS1-1 is found to display a novel multistate unfolding/refolding pathway involving a partially active dimeric intermediate and an inactive monomeric intermediate (i.e., $N_2 \leftrightarrow I_2 \leftrightarrow 2M \leftrightarrow 2U$).

EXPERIMENTAL PROCEDURES

Materials. Squid GSTS1-1 was overexpressed in *E. coli* BL21(DE3) transformed with the plasmid GST5/pET, purified by *S*-hexylglutathione (S-hexylGSH) affinity chromatography as described (*8*), and stored in 20 mM sodium phosphate buffer, pH 7, 0.1 M NaCl, 1 mM EDTA, 5 mM dithiothreitol (DTT). Protein was eluted from the affinity matrix either with 2 mM S-hexylGSH (which was subsequently removed by filtration through Sephadex G-25) or with 10 mM glycine, pH 10 (*18*). Similar unfolding results were obtained with either protein preparation. The protein concentration of the dimer was determined using an extinction coefficient of 31 660 M^{-1} cm^{-1} at 280 nm (*19*). Ultrapure urea was purchased from ICN, guanidinium chloride (GdmCl) was from BDH, and 1-chloro-2,4-dinitrobenzene (CDNB) and 8-anilino-1-naphthalenesulfonate (ANS) were purchased from Sigma. DTT and reduced glutathione (GSH) were purchased from Boehringer Mannheim. S-HexylGSH was prepared as described (*20*). All other chemicals were of analytical grade.

Equilibrium Unfolding. All unfolding experiments were performed in 20 mM sodium phosphate buffer, pH 7, 1 mM EDTA, 5 mM DTT, and at various concentrations of NaCl (0−1 M). Protein (final concentration of 1 μM) was incubated with urea (0−6 M) or GdmCl (0−6 M) and allowed to reach equilibrium (>4 h) at 20 °C. For determining the effect of GSH and S-hexylGSH on unfolding, the protein was incubated with the ligand for 30 min before the addition of denaturant. Unfolding was found to be highly reversible following a 10-fold dilution of the denaturant; i.e., recoveries for renatured protein were >95% for tryptophan fluorescence and >77% for enzyme activity. The formation of protein aggregates during unfolding/refolding was monitored by light scattering using excitation and emission wavelengths of 295 nm. No aggregation was detected for all the results shown.

The conformational stability parameters $\Delta G(H_2O)$ (the difference in Gibbs free energy between folded and unfolded protein) and the *m*-value (the dependence of the free energy of unfolding upon denaturant concentration) were calculated from unfolding transitions by the linear extrapolation method (*21*, *22*) as described (*15*). Values for C_m (the denaturant concentration at which half of the population of protein molecules are unfolded) were obtained from the midpoints of the unfolding transitions.

Fluorescence Spectroscopy. Fluorescence measurements were made with a Hitachi 850 fluorescence spectrophotometer using excitation and emission band-passes of 5 or 10 nm. The temperature of the cuvette holder was controlled using a circulating thermostated water bath. Fluorescence values were corrected for appropriate blanks. An excitation wavelength of 295 nm was used to selectively excite tryptophans. Results are shown as the ratio of fluorescence intensity at 355 nm (emission maximum for denatured protein) to the fluorescence intensity at 330 nm (emission maximum for native protein in 0.1 M NaCl at 20 °C), thereby indicating the extent of unfolding. For the protein concentration dependence study, an excitation wavelength of 280 nm was used to improve the fluorescence signal (emission wavelengths of 320 and 355 nm for native and unfolding protein, respectively). Excitation at 280 nm yielded similar unfolding transitions to those observed using 295 nm excitation.

Steady-state anisotropy was measured using Hitachi polarization accessories. Measurements were made with an excitation wavelength of 295 nm and an emission wavelength of 355 nm. The fluorescence intensities I_{VV} and I_{VH} were monitored where V (vertical) and H (horizontal) refer to the polarization of the excitation and emission light, respectively. Anisotropy was calculated as follows (*23*):

$$A = (I_{VV} - GI_{VH})/(I_{VV} + 2GI_{VH})$$

where $G = I_{HV}/I_{HH}$. G corrects for the different efficiencies of the monochromators for horizontally and vertically polarized light ($G = 1.07$).

Enzyme Activity. Enzyme activity was measured spectrophotometrically at 340 nm using 0.67 nM protein with 1

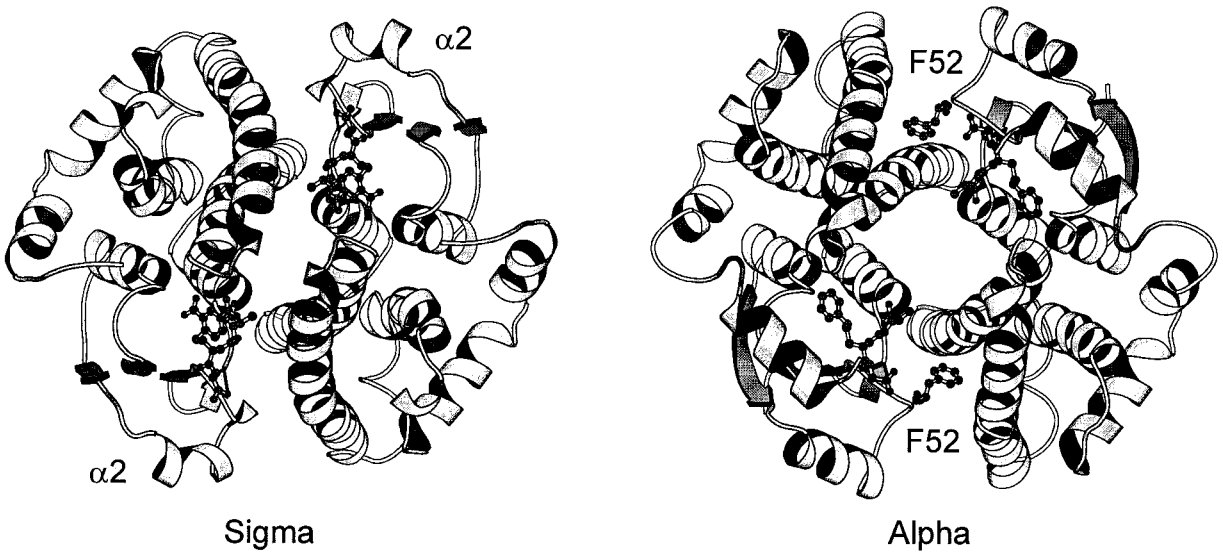

FIGURE 1: Ribbon representations of the class sigma (*8*) and alpha (*11*) glutathione transferases down the dimer 2-fold axis. The side chain of F52 in one subunit of the class alpha protein, shown in a ball-and-stick representation, intercalates between α-helices 4 and 5 in the other subunit. This hydrophobic intersubunit lock-and-key interaction is absent in the class sigma protein. The location of α-helix 2, which contains the single tryptophan (W38), is shown. The active-site ligands are shown as ball-and-stick representations. The diagrams were generated using the program MOLSCRIPT (*12*).

mM GSH and 1 mM CDNB in 0.1 M potassium phosphate buffer, pH 6.5, 3% ethanol at room temperature (*24*). Aliquots of protein were added to the assay mixture and assayed over 1 min. Reactivation within this time, due to renaturation, was found to be less than 10%. All assays were corrected for nonenzymatic rates.

ANS Binding. ANS in 20 mM sodium phosphate buffer, pH 7, was added to a final concentration of 200 μM to protein equilibrated with denaturant. The binding of the ligand was monitored by direct excitation at 400 nm and emission measured at 480 nm. All intensities were corrected for blanks.

Size-Exclusion HPLC. An analytical BIOSEP SEC-S3000 size-exclusion column (Phenomenex) and a flow rate of 0.5 mL/min were used to determine the hydrodynamic volume of the protein as it unfolds (*14*). Protein was detected by absorbance at 280 nm, and retention times were determined for protein equilibrated in different concentrations of urea on the column which was equilibrated in the same urea concentration.

Circular Dichroism. Circular dichroism was measured using a Jasco J-710 spectropolarimeter, with a 1 mm path length in a 10 mM sodium phosphate buffer, pH 7, 1 M NaCl. The spectra are an average of 16 runs.

RESULTS

Probes. A variety of probes were used to monitor structural changes during the unfolding/refolding of squid GSTS1-1. Each subunit of GSTS1-1 has a single tryptophan residue (Trp38) which is located in α-helix 2 of domain I (Figure 1). Its close proximity to the active site and involvement in sequestering the substrate glutathione make it a sensitive fluorescence probe to monitor conformational changes at/near the active site and in α-helix 2. Enzyme activity provides an indication of the conformation of domain I as well as the subunit interface due to the involvement of Asp96 from the adjacent subunit in forming a fully functional active site. The binding of the amphipathic dye ANS is used to determine the exposure of hydrophobic regions and formation of compact hydrophobic states during unfolding (*25*−*27*). Changes in the hydrodynamic volume of GSTS1-1 were monitored by steady-state anisotropy and size-exclusion HPLC. These probes monitor primarily tertiary and quaternary structure. Far-ultraviolet circular dichroism (far-UV CD) was used to monitor the disruption of protein secondary structure.

Urea-Induced Equilibrium Unfolding and Effect of NaCl. Replicates of at least three unfolding curves obtained on different days and/or from different protein preparations indicate the high reproducibility of all unfolding/refolding data. The unfolding of GSTS1-1 at 20 °C required the presence of at least 0.4 M NaCl to prevent protein aggregation within the unfolding transition. Figure 2 shows unfolding curves for GSTS1-1 at 20 °C/0.4 M NaCl obtained with intrinsic tryptophan fluorescence and enzyme activity (Figure 2A), and ANS binding and anisotropy (Figure 2B). At 0.4 M NaCl, the tryptophan fluorescence transition is biphasic. The emission maximum of Trp38 shifts from 337 to 345 nm in the first fluorescence phase (0−1.8 M urea) as the fluorescence becomes partially exposed and then from 345 to 355 nm during the second fluorescence phase (>1.8 M urea) as the protein unfolds completely (confirmed by circular dichroism). Toward the end of the first fluorescence transition, there is a 20−30% reduction in enzyme activity. The ANS binding probe, however, demonstrates that there is an additional unfolding event that only starts to occur from about 1 M urea and peaks at 1.8 M urea. The left side of the ANS binding peak coincides with a complete loss of enzyme activity (1−1.8 M urea), whereas the right side of the peak coincides with the second fluorescence phase (1.8−4 M urea; midpoint at about 2.7 M). The anisotropy signal also coincides with the second fluorescence phase, indicating a major change in the protein's hydrodynamic volume in this concentration range (see inset to Figure 2B).

The presence of NaCl impacts markedly on the emission maximum of Trp38 in that it shifts from 330 to 342 nm as

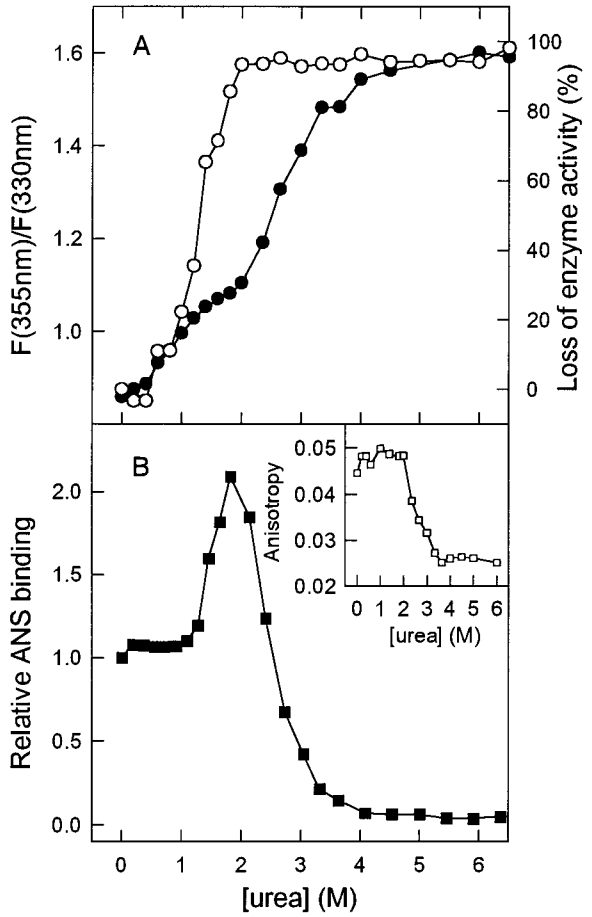

FIGURE 2: Urea unfolding of GSTS1-1 in 0.4 M NaCl at 20 °C. 1 μM protein in 20 mM sodium phosphate, 1 mM EDTA, 5 mM DTT, pH 7, was equilibrated at different urea concentrations. Unfolding was monitored by tryptophan fluorescence (●), expressed as the ratio of the fluorescence at 355 nm to the fluorescence at 330 nm (excitation at 295 nm) and enzyme activity (○) as shown in (A). (B) shows the binding of the ligand ANS (■) which was monitored by direct excitation (400 nm) and emission at 480 nm (arbitrary units) following the addition of 200 μM ANS to protein equilibrated at different urea concentrations. The inset in (B) shows the steady-state fluorescence anisotropy (□) which was measured using an excitation wavelength of 295 nm and an emission wavelength of 355 nm.

the concentration of NaCl is increased from 0.1 to 1 M. This suggests an ionic-strength-induced conformational change in GSTS1-1 that causes Trp38 to move into a less hydrophobic environment. When the NaCl concentration was increased from 0.4 to 1 M, the unfolding transition monitored by tryptophan fluorescence became triphasic (Figure 3A) whereas the activity transition appears to become biphasic (Figure 3B). ANS binding remains as a single peak (Figure 3C) (the open and closed symbols in Figure 3 are for 0.1 and 1 μM GSTS1-1, respectively; protein concentration dependence will be dealt with below). Increasing NaCl shifts the first fluorescence phase slightly toward lower urea concentrations but shifts the final fluorescence phase substantially toward higher urea concentrations (i.e., from a midpoint of 2.7 M urea for 0.4 M NaCl to 3.5 M urea for 1 M NaCl). The cooperativity of unfolding/refolding for this phase (i.e., the slope) appears, however, not to be affected. This was confirmed by the *m*-value of about 2.2 kcal mol^{-1} M^{-1} for both phases. The stability parameter $\Delta G(H_2O)$, however,

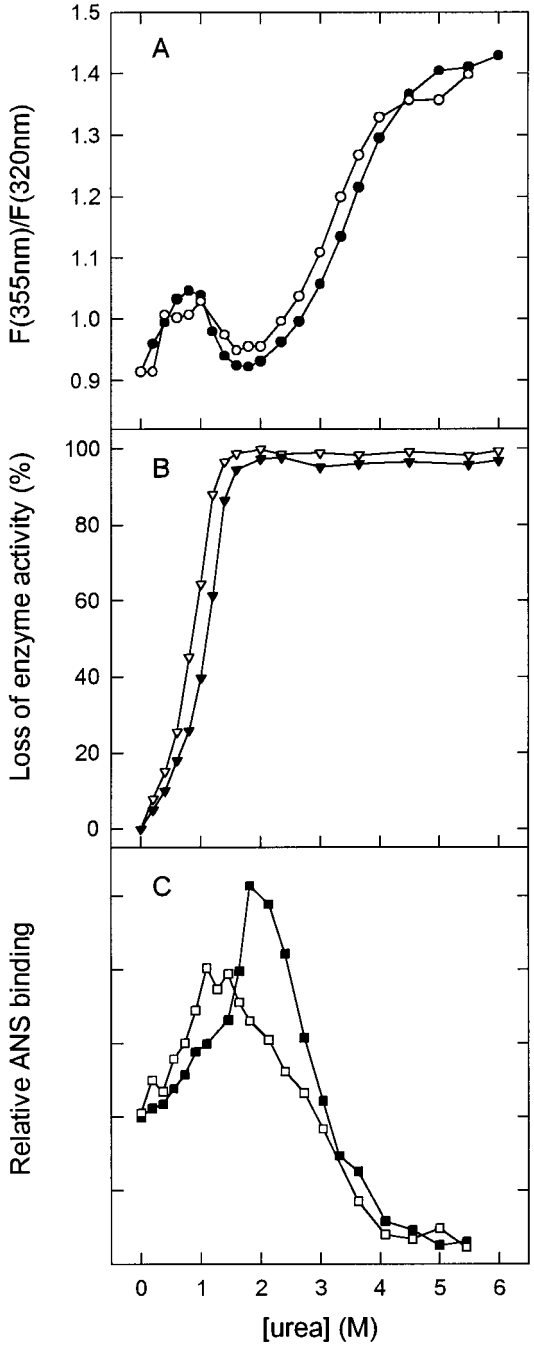

FIGURE 3: Urea unfolding of GSTS1-1 in 1 M NaCl at 20 °C. Protein at concentrations of 0.1 μM (hollow symbols) and 1 μM (filled symbols) in 20 mM sodium phosphate, 1 mM EDTA, 5 mM DTT, pH 7, was equilibrated at different urea concentrations. Unfolding was monitored by tryptophan fluorescence (●), expressed as the ratio of the fluorescence at 355 nm to the fluorescence at 330 nm (excitation at 295 nm) as shown in (A). (B) shows the loss of enzyme activity (▼), and (C) shows the binding of ANS (■) which was monitored by direct excitation (400 nm) and emission at 480 nm (arbitrary units) following the addition of 200 μM ANS to protein equilibrated at different urea concentrations.

increased from about 12.5 kcal mol^{-1} (at 0.4 M NaCl) to about 15.5 kcal mol^{-1} (at 1 M NaCl).

In the presence of 1 M NaCl, the emission maximum of Trp38 shifts from 342 to 347 nm during the first fluorescence phase (0−0.8 M urea), indicating a partial exposure of the fluorophore. It then shifts back to 342 nm during the second phase (0.8−1.8 M urea), indicating the movement of Trp38

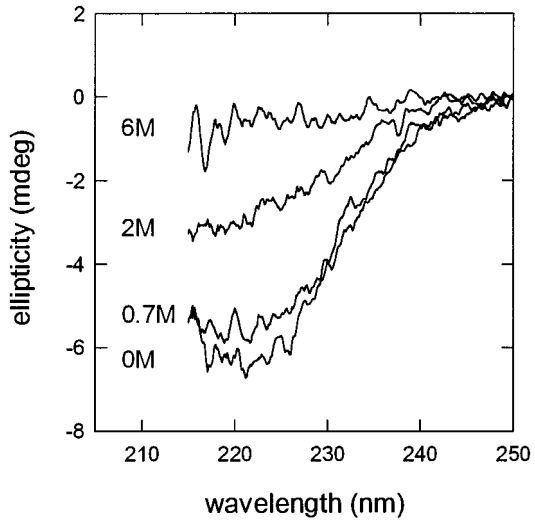

FIGURE 4: Far-UV circular dichroism spectra of GSTS1-1 in different urea concentrations (indicated on the left of the spectra). Protein concentration was 1 μM in 10 mM sodium phosphate buffer, pH 7, 1 M NaCl. The wavelength range was limited to 215 nm due to interference of NaCl and urea at lower wavelengths.

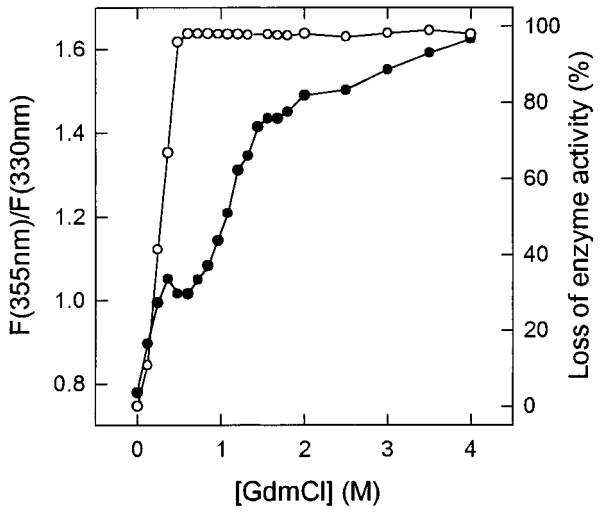

FIGURE 5: Unfolding of GSTS1-1 by guanidinium chloride 1 μM protein in 20 mM sodium phosphate, 1 mM EDTA, 5 mM DTT, pH 7, was equilibrated at different concentrations of guanidinium chloride at 20 °C. Unfolding was monitored by the tryptophan fluorescence (●), expressed as the ratio of the fluorescence at 355 nm to the fluorescence at 330 nm (excitation at 295 nm), and loss of enzyme activity (○).

back into a more hydrophobic environment. The third and final fluorescence phase corresponds to Trp38 becoming fully exposed to solvent (shifts from 342 to 355 nm) upon complete unfolding.

When native GSTS1-1 binds ANS, the dye's emission maximum shifts from 535 nm for unbound dye to 495−500 nm for bound dye, demonstrating that the dye binds a hydrophobic region. The enhanced ANS binding during the unfolding process (as shown in Figures 2B and 3C) was accompanied by a blue shift in the emission maximum for protein-bound ANS from 500 nm (0 M urea) to 480 nm (1.8−2 M urea), demonstrating that the binding environment became even more hydrophobic. Furthermore, the apparent dissociation constant (K_d) for ANS decreased from 83 μM (0 M urea) to 28 μM (2 M urea), confirming increased capacity/tighter binding of the dye.

To determine the secondary structure of the different protein conformations, far-UV CD spectra were collected and are shown in Figure 4. The native protein shows a trough at 222 nm as would be expected for a predominantly α-helical protein. The spectrum for protein in 0.7 M urea shows a small change in the secondary structure in the characteristic region for α-helices; 0.7 M urea in 1 M NaCl results in a 25% inactivation of the protein and precedes the major enhancement in ANS binding. The spectrum for GSTS1-1 in 2 M urea shows a more substantial loss in secondary structure with less than half of the native ellipticity at 222 nm. The spectrum for 6 M urea confirms that the protein is unfolded under these conditions, and approximates a random coil conformation.

Size-Exclusion HPLC. Size-exclusion chromatography can be employed to study protein unfolding due to its ability to resolve changes in the hydrodynamic properties of structures along an unfolding pathway, and to detect the presence of intermediate states provided they are kinetically stable within the time scale of the chromatographic run (*28*). This technique has been applied successfully to other GSTs (*14*, *15*). In this study, the hydrodynamic volume of GSTS1-1 did not change significantly between 0 and 1.0 M, urea confirming that the protein behaves as a dimer within this urea concentration range (data not shown). At higher urea concentrations (>1−4 M urea), the recovery of protein from the column was very poor (as monitored by a loss in the absorbance signal at 280 nm), indicating that the protein adsorbed to the column. This would be expected in this urea concentration range because of increased surface hydrophobicity (as displayed by enhanced ANS binding).

Protein Concentration Dependence of Unfolding. Since GSTS1-1 is a homodimer, its equilibrium unfolding pathway starting with the native dimer and ending with unfolded monomers should possess a protein concentration dependent dissociation step. From initial experiments at 0.4 M NaCl with 0.1−1 μM protein (higher protein concentrations could not be used because of aggregation and lower concentrations yielded poor signals), it was not possible to identify the protein concentration dependent phase as all the transitions appeared to be protein concentration independent. However, at 1 M NaCl, which improved the resolution between the different transitions (see Figure 3 as compared with Figure 2), there was a substantial shift in the ANS-binding peak (Figure 3C) to higher urea concentrations as the protein concentration increased. This indicates that this probe is most sensitive to detecting the dissociation step. The small shift in the enzyme activity transition with a change in protein concentration is expected, as activity is affected by dissociation (as well as the formation of the dimeric intermediate). The tryptophan fluorescence transitions did not show a significant shift for the different protein concentrations (Figure 3A), indicating that it is not a sensitive probe for detecting the dissociation of the dimeric state of GSTS1-1. In addition, the anisotropy was not sensitive to the dissociation step but was very sensitive toward the major unfolding event occurring at higher urea concentrations (see Figure 2B, inset). The bimolecular dissociation step is, therefore, situated between two unimolecular unfolding steps.

Effect of an Ionic Denaturant and Thermal Denaturation. The data in Figure 5 show that the strong ionic denaturant

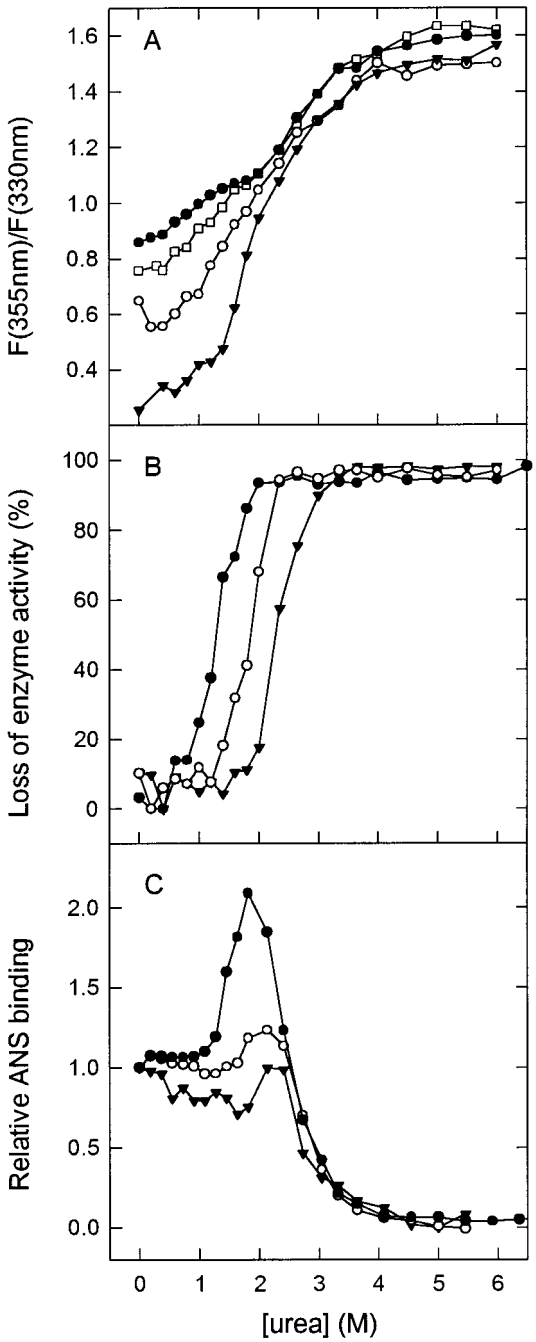

FIGURE 6: Effect of active-site ligands on urea unfolding of GSTS1-1 in 0.4 M NaCl at 20 °C. 1 μM protein was preincubated with different concentrations of GSH or S-hexylGSH (●, no ligand; □, 2 mM GSH; ○, 10 mM GSH; ▼, 1 mM S-hexylGSH) for 30 min in 20 mM sodium phosphate, 1 mM EDTA, 5 mM DTT, pH 7, and then equilibrated at different urea concentrations. Unfolding was monitored by tryptophan fluorescence (A) expressed as the ratio of the fluorescence at 355 nm to the fluorescence at 330 nm (excitation at 295 nm), enzyme activity (B), and binding of ANS (C) which was monitored by direct excitation (400 nm) and emission at 480 nm (arbitrary units) following the addition of 200 μM ANS to protein equilibrated at different urea concentrations.

GdmCl unfolds GSTS1-1 in the same manner as observed with urea. The thermostability of GSTS1-1 was determined by following its melting curves using enzyme activity and tryptophan fluorescence (data not shown). Changes in both started to occur just above 20 °C, but the protein began to aggregate irreversibly from about 38 °C. A relatively low melting temperature (T_m) of 35 °C determined from the enzyme activity melting curve confirms that GSTS1-1 is heat-labile.

Effect of Glutathione and S-Hexylglutathione on Unfolding. Each subunit of GSTS1-1 has an active site consisting of a G-site (glutathione-binding site) and an adjacent H-site (for the hydrophobic electrophilic substrate) (*6*). Figure 6 shows the effect that the binding of the active site ligands glutathione and *S*-hexylglutathione has on the urea-induced unfolding transitions of GSTS1-1 at 20 °C/0.4 M NaCl. The binding of these ligands to the enzyme causes a substantial reduction in the first fluorescence phase without much effect on the second fluorescence phase. This was accompanied by a shift in the enzyme's activity (Figure 6B) and ANS-binding peak (Figure 6C) toward higher urea concentrations. These data support a stabilization of the native state of GSTS1-1 upon occupation of its active sites, a phenomenon observed for other GSTs (*29*, W. J. Parsons and H. W. Dirr, unpublished results). The reduction in the size of the ANS-binding peak results from the shift of the unfolding transition for the more stable protein−ligand complex toward higher urea concentrations at which the ANS-binding intermediate is less stable. The greater effects observed with the lower concentration of S-hexylGSH can be explained by its higher affinity for the protein; its apolar hexyl moiety increases the number of interactions with the protein's active site. Furthermore, neither 10 mM GSH nor 1 mM S-hexylGSH had any impact on ANS binding in the absence of urea (K_d about 83 μM) or in the presence of 2 M urea (K_d about 28 μM).

In the absence of urea, the enzyme's emission maximum was markedly blue shifted from 337 nm (no ligand) to 325 nm with 1 mM S-hexylGSH (as reflected in the lower fluorescence ratios seen at 0 M urea in Figure 6A). Occupation of the G-site appears, therefore, to induce a significant conformational change in the native protein structure near Trp38 which causes the fluorophore to move into a more hydrophobic environment.

DISCUSSION

Unfolding Pathway for Class Sigma GSTS1-1. The overall unfolding pathway for a homodimeric protein must begin with a folded dimer (N_2) and end with two unfolded monomers (2U). This can be achieved in several ways, three of which are described below as examples:

$$\text{model 1: } N_2 \leftrightarrow 2U$$

For this basic model in which only folded dimer and unfolded monomer are highly populated at equilibrium, monophasic and coincident unfolding curves are expected at a fixed protein concentration. Furthermore, since this two-state model represents a concerted and bimolecular dissociation/unfolding reaction, it should be protein concentration dependent (*3*):

$$\text{model 2: } N_2 \leftrightarrow 2N \text{ (or } 2I) \leftrightarrow 2U$$

$$\text{model 3: } N_2 \leftrightarrow I_2 \leftrightarrow 2U$$

For models 2 and 3, where N_2 is native dimer, N is native monomer, I is a monomeric intermediate, I_2 is a dimeric intermediate, and U is unfolded monomer, one expects biphasic unfolding curves and/or noncoincident transitions

if the probes used can differentiate between the different conformational states. The dependence of the unfolding behavior upon protein concentration can be used as a definitive diagnostic tool to distinguish between the two three-state mechanisms; i.e., only the bimolecular dissociation steps (the first and second steps in models 2 and 3, respectively) should be protein concentration dependent.

In this study, the unfolding data demonstrate that the probes used are differentially sensitive to various conformational states of GSTS1-1. The presence of multiple and nonsuperimposable transitions for GSTS1-1 indicates that a simple two-state unfolding process involving only native dimer and unfolded monomer is not applicable but is highly suggestive of the existence of two well-populated stable intermediates. The first unfolding transition from native dimer to a dimeric intermediate was confirmed by its protein concentration independence. The dimeric nature of the intermediate was further confirmed by size-exclusion chromatography at urea concentrations where the intermediate is well-populated. The dimeric intermediate is partially inactive (20−30%) as seen by the activity transitions which show the combined effect of the partial unfolding producing the dimeric intermediate and the dissociation into the monomeric state. The CD spectrum of the dimeric intermediate (0.7 M urea) shows that a small change in secondary structure is involved in the formation of this state. The second unfolding transition is protein concentration dependent, indicative of the presence of the dissociation of the dimeric intermediate to two monomeric intermediates. The secondary structure of the monomeric intermediate is substantially different from the native state, but it does retain significant structural content as confirmed by the ability to bind ANS. The third transition is a protein concentration independent unfolding of the monomeric intermediate, which is confirmed by the CD spectrum.

The native dimer and partially active dimeric intermediate have similar ANS binding properties, suggesting that the nonsubstrate ligand-binding site for ANS located at the center of the dimer interface of cytosolic GSTs (*30*) is not disrupted. The equilibrium between native dimer and dimeric intermediate is shifted toward the intermediate with increasing ionic strength whereas the binding of ligands to the enzyme's active site stabilizes the native dimer. The catalytically inactive monomeric intermediate displays increased hydrophobicity and affinity/capacity for binding ANS, and its conformational stability is enhanced with increasing NaCl concentration. This monomeric state has some properties in common with a molten globule, such as compactness and enhanced ANS binding (*1*). The experimental *m*-value of 2.2 kcal mol^{-1} M^{-1} obtained for the third unfolding transition correlates very well with the amount of protein surface area expected to become exposed upon unfolding for a monomeric state of GSTS1-1. The change in accessible surface area, ΔASA, for a monomer of 202 amino acids is 17 900 $Å^2$ while for a dimer of 404 residues it is 36 700 $Å^2$ (*31*). From these ΔASA data, *m*-values of 2.35 and 4.43 kcal mol^{-1} M^{-1}, respectively, were calculated (*31*). Experimentally obtained *m*-values for class pi (*14*), class alpha (*16*), and schistosomal (*15*) GSTs compare well with values calculated from (*31*), suggesting that the size of the protein or the amount of its surface area exposed to solvent upon unfolding is the major structural determinant for the *m*-value.

In addition to the properties discussed above, tryptophan fluorescence indicates nonidentical tertiary structures for the monomer in the native dimer, intermediate dimer, and monomeric intermediate. Fluorescence intensity and emission maximum values differ for the three states. Trp38 is in a hydrophobic environment in the native dimer (λ_{max} 330 nm at low NaCl), whereas it is in a polar environment in the dimeric (λ_{max} 347 nm) and monomeric (λ_{max}342 nm) intermediates. Studies are underway to characterize the two intermediate states further.

The results from this study, therefore, are strongly supportive of the following four-state pathway for class sigma GSTS1-1:

$$N_2 \leftrightarrow I_2 \leftrightarrow 2M \leftrightarrow 2U$$

This pathway is unique for the cytosolic GSTs for which two-state pathways involving folded dimer and unfolded monomers have been observed for class pi (*13*, *14*), schistosomal (*15*), and class alpha (*16*) GSTs. Furthermore, their higher C_m values of about 4.5 M urea and T_m-values of about 55 °C are consistent with their greater thermodynamic stability [$\Delta G(H_2O)$ values range from 20 to 27 kcal mol^{-1} M^{-1}]. Because of the lack of well-defined pre- and post-transitions for the class sigma GST and because none of the probes are uniquely sensitive to any one of the transitions, it was not possible to fit the data and determine thermodynamic parameters for all the transitions.

Cytosolic GSTs can be grouped according to the features at their subunit interfaces. The class alpha/mu/pi/schistosomal group have a prominent hydrophobic lock-and-key type interaction at each end of the subunit interface, the key being a phenylalanine/tyrosine side chain in domain I of one subunit and the lock being a hydrophobic pocket in domain II of the other subunit (*8* and references cited therein). On the other hand, GSTs in the class sigma/theta group (e.g., the squid GSTS1-1) lack this interaction, and their subunit interfaces are more hydrophilic. Protein engineering studies are in progress to establish what role these structural features may play in determining GST stability and folding. The dependence of the stability of GSTS1-1 upon ionic strength suggests an important role for electrostatic forces. Polar interactions predominate at the subunit interface of GSTS1-1, and their solvation by water and/or shielding by salt during unfolding most likely affects subunit association and facilitates the formation of a stable monomeric intermediate. The absence of stable monomeric states along the unfolding pathways of class alpha/mu/pi/schistosomal GSTs could be due to the predominantly hydrophobic nature of their subunit interfaces that would be unstable when exposed to solvent.

Structurally, GSTS1-1 has a very exposed active site giving rise to a highly catalytically efficient GST (*8*). Located at this site is α-helix 2 which is solvent-exposed and flexible (the latter implied by its above-average temperature factors). Although this region is flexible throughout the superfamily, the absence of the hydrophobic lock-and-key interaction across the subunit interface of GSTS1-1 would most likely diminish the stability of α-helix 2 further. The binding of glutathione/glutathione analogues to the active site should reduce this flexibility of α-helix 2 and stabilize domain I. Although no crystal structure is available at present for uncomplexed GSTS1-1, there is crystallographic

evidence for the stabilization of this region in the murine class pi GSTP1-1 (*32*). The observed loss of electron density in its α-helix 2 region is regained when the class pi enzyme is complexed with glutathione analogues. This supports the suggestion above that a region at/near the G-site of GSTS1-1 (most likely its α-helix 2 region) is unstable and unfolds at low denaturant concentrations (0−0.8 M urea) forming a dimeric intermediate with increased solvent exposure of Trp38 located in α-helix 2. This explanation is consistent with the small change in α-helical content shown by the CD spectrum for the dimeric intermediate which results in a loss of activity.

Implications for Evolutionary Selection of Class Sigma GST as a Crystallin. The proposed evolutionary development of GSTs is thought to have occurred from a class theta ancestor with the class sigma diverging before any of the vertebrate classes (*8*, *33*). This class sigma GST is then proposed to have been selected by evolution as a soluble refractory protein, or lens crystallin, in cephalopods, which have highly developed eyes (*17*). It shows a higher sequence identity to S-crystallins of the squid and octopus (42−44%) than to GSTs of other gene classes (19−34%) (*8*). Crystallins are required to have high thermodynamic stability because of the low protein turnover in the fiber cells in the eye lens. In many cases in vertebrates and invertebrates these proteins have been recruited from proteins with existing functions, such as the δ-crystallin (argininosuccinate lyase), τ-crystallin (α-enolase), and L-crystallin (aldehyde dehydrogenase), as reviewed (*34*). A GST would be an ideal crystallin candidate because of possible detoxification and oxidative stress-protective functions in the lens, as well as high solubility. However, the requirement for stability in the class sigma GST does not appear to be met. The protein has been shown to be highly susceptible to thermal and solvent-induced denaturation. This could explain why this type of GST survived selective pressure during molecular evolution only in cephalopods and has not been found in vertebrates, neither as a detoxification protein nor as a crystallin. Selective pressures in the cephalopod environment are clearly different from those for some other organisms (variations in pressure, temperature, and light intensity) which may account for this incongruity. Unfolding kinetics studies have shown that the class sigma GST unfolds slowly, which may have contributed to the selection as a crystallin (unpublished data). Little is know about the stability of invertebrate crystallins at present, but studies are underway to characterize the folding and stability of the S-crystallin to which the class sigma GST is most closely related (SL11). This will determine the effect of the structural changes which have caused a major loss of the catalytic activity of the crystallin, as well as if the crystallin is more stable than the GST from which it was derived.

REFERENCES

1. Ptitsyn, O. (1995) *Adv. Protein Chem. 47*, 83−229.
2. Privalov, P. L. (1992) in *Protein Folding* (Creighton, T. E., Ed.) pp 83−126, W. H. Freeman and Co., New York.
3. Neet, K. E., and Timm, D. E. (1994) *Protein Sci. 3*, 2167−2174.
4. Armstrong, R. N. (1991) *Chem. Res. Toxicol. 4*, 131−140.
5. Listowsky, I. (1993) in *Hepatic transport and bile secretion: physiology and pathophysiology* (Tavoloni, N., and Berk, P., Eds.) pp 397−405, Raven Press, New York.
6. Dirr, H. W., Reinemer, P., and Huber, R. (1994) *Eur. J. Biochem. 220* 645−661.
7. Pemble, S. E., Wardle, A. F., and Taylor, J. B. (1996) *Biochem. J. 319*, 749−754.
8. Ji, X., von Rosenvinge, E. C., Johnson, W. W., Tomarev, S. I., Piatigorsky, J., Armstrong, R. N., and Gilliland, G. L. (1995) *Biochemistry 34*, 5317−5328.
9. Meyer, D. J., Coles, B., Pemble, S. E., Gilmore, K. S., Fraser, G. M., and Ketterer, B. (1991) *Biochem. J. 274*, 409−414.
10. Wilce, M. C. J., and Parker, M. W. (1994) *Biochem. Biophys. Acta 1205*, 1−18.
11. Sinning, I., Kleywegt, G. L., Cowan, S. W., Reinemer, P., Dirr, H. W., Huber, R., Gilliland, G. L., Armstrong, R. N., Ji, X., Board, P. G., Olin, B., Mannervik, B., and Jones, T. A. (1993) *J. Mol. Biol. 232*, 192−212.
12. Kraulis, P. J. (1991) *J. Appl. Crystallogr. 24*, 946−950.
13. Dirr, H. W., and Reinemer, P. (1991) *Biochem. Biophys. Res. Commun. 180*, 294−300.
14. Erhardt, J., and Dirr, H. W. (1995) *Eur. J. Biochem. 230*, 614−620.
15. Kaplan, W., Hüsler, P., Klump, H., Erhardt, J., Sluis-Cremer, N., and Dirr, H. W. (1997) *Protein Sci. 6*, 399−406.
16. Wallace, L., Sluis-Cremer, N., and Dirr, H. W. (1998) *Biochemistry 37*, 5320−5328.
17. Tomarev, S. I., and Zinovieva, R. D. (1988) *Nature 336*, 86−88.
18. Cameron, A. D., Sinning, I., L'Hermite, G., Olin, B., Board, P. G., Mannervik, B., and Jones, T. A. (1995) *Structure 3*, 717−727.
19. Perkins, S. J. (1986) *Eur. J. Biochem. 157*, 169-180.
20. Vince, R., Daluge, S., and Wadd, W. B. (1971) *J. Med. Biochem. 14*, 402−404.
21. Pace, C. N. (1986) *Methods Enzymol. 131*, 266−280.
22. Schellman, J. A. (1978) *Biopolymers 17*, 1305−1322.
23. Lacowicz, J. R. (1983) *Principles of fluorescence spectroscopy*, pp 112−151, Plenum Press: New York.
24. Habig, W. H., and Jakoby, W. B. (1981) *Methods Enzymol. 77*, 398−405.
25. Semisotnov, G. V., Rodionova, N. A., Kutyshenko, V. P., Ebert, B., Blank, J., and Ptitsyn, O. B. (1987) *FEBS Lett. 224*, 9−13.
26. Lindsay, C. D., and Pain, R. H. (1990) *Eur. J. Biochem. 192*, 133−141.
27. De Young, L. R., Dill, K. A., and Fink, A. L. (1993) *Biochemistry 32*, 3877−3886.
28. Corbett, R. J. T., and Roche, R. S. (1984) *Biochemistry 23*, 1888−1894.
29. Erhardt, J., and Dirr, H. W. (1996) *FEBS Lett. 391*, 313−316.
30. Sluis-Cremer, N., Naidoo, N. N., Kaplan, W. H., Manoharan, T. H., Fahl, W. E., and Dirr, H. W. (1996) *Eur. J. Biochem. 241*, 484−488.
31. Myers, J. K., Pace, C. N., and Scholtz, J. M. (1995) *Protein Sci. 4*, 2138−2148.
32. Vega, M. C., Walsh, S. B., Mantle, T. J., and Coll, M. (1998) *J. Biol. Chem. 273*, 2844−2850.
33. Pemble, S. E., and Taylor, J. B. (1992) *Biochem. J. 287*, 957−963.
34. Tomarev, S. I., and Piatigorsky, J. (1996) *Eur. J. Biochem. 235*, 449−465.

BI981044B